52
Research paper
Doi 10.61892/STP202601055M
ISSN 2566-4484

STEPGRAD
СТЕПГРАД

Miroslav Marjanović, University of Belgrade, mmarjanovic@grf.bg.ac.rs

STATIC AND DYNAMIC ANALYSIS OF CLT-CONCRETE COMPOSITES USING LAYERED FINITE ELEMENTS

Abstract:

In the paper, a layerwise formulation of cross-laminated-timber (CLT) - concrete composites (CCC) is presented. A partial shear interaction between concrete and CLT is incorporated by using distributed elastic springs in the CLT-concrete interface. A linear discontinuous layerwise interpolation of displacement components through the thickness is imposed to account for layerwise kinematics with partial shear connection. The model accuracy is demonstrated against the available data in the literature, using benchmark examples including both static and dynamic analysis, and excellent agreement is obtained with computational cost savings.

Keywords: timber-concrete composite, cross-laminated timber, layered finite element

СТАТИЧКА И ДИНАМИЧКА АНАЛИЗА СПРЕГНУТИХ ПЛОЧА CLT-БЕТОН ПРИМЕНОМ СЛОЈЕВИТИХ КОНАЧНИХ ЕЛЕМЕНАТА

Резиме:

У раду је приказана формулација композита од унакрсно-ламелираног дрвета (CLT) и бетона (CCC), заснована на слојевитој теорији плоча. Парцијална интеракција између бетона и CLT-а је узета у обзир применом површинских еластичних опруга на контакту CLT-а и бетона. Примењена је линеарна дисконтинуална слојевита интерполација померања по дебљини плоче, како би се у обзир узела кинематика слојевитог композита са парцијалним смичућим спојем. Тачност модела је потврђена у односу на доступне резултате у литератури, на примерима статичке и динамичке анализе. Добијено је одлично поклапање резултата уз смањено трајање прорачуна.

Кључне речи: композит дрво-бетон, унакрсно-ламелирано дрво, слојевити коначни елемент

1. INTRODUCTION

The advantages of cross-laminated timber (CLT) in the construction sector are primarily associated with its low environmental impact, high mechanical efficiency, ease of prefabrication, and rapid erection [1]. CLT provides excellent stiffness-to-weight ratio, allowing the application of such panels as full-size walls or floors [2]. In recent years, CLT–concrete composites (CCC) have gained widespread application in floor systems due to their superior structural performance, including high stiffness, bending resistance, favorable dynamic behavior, and enhanced acoustic and thermal insulation properties [3]. They represent a promising alternative to conventional reinforced concrete (RC) floors in medium- and high-rise buildings and constitute a natural evolution of timber–concrete composite (TCC) systems [4].

In both TCC and CCC, the timber and concrete layers are interconnected using different connection systems, such as notched shear connectors, screwed connectors, dowel-type fasteners, adhesives, rods, shear studs, or their combinations [5], [6]. The selection of connection type is particularly important because it governs the structural rigidity under service load, and affects both the vibration performance and stiffness during a fire. Significant research efforts have been devoted so far to predicting the slip modulus and shear capacity of the screw-type connections, associated with concrete and timber thicknesses or mechanical properties and various screw sizes, layouts and penetration lengths. Extensive experimental programs followed by the development of analytical solutions for the prediction of slip modulus and interlayer slip have been conducted so far [7], [8], [9], [10].

CLT floors and their composite variants are susceptible to excessive vibrations caused by human activities [11], which are the most common vibration sources in residential and commercial buildings. Excessive vibrations can be detrimental to occupants' comfort or may cause malfunctions of vibration-sensitive equipment [12]. Consequently, design of long-span open-plan CLT floors is commonly governed by vibration serviceability requirements rather than ultimate limit state or deflection limitations [13], [14]. This necessitates the development of accurate computational models, which may account for specifics of such structures, such as transverse shear deformation and partial shear connection at the interface.

Most existing computational models for predicting the static and dynamic behavior of CCC structures are based on simplified beam-type formulations, which are limited in their ability to represent two-dimensional load transfer and cannot adequately capture the plate-like behavior of such systems [15]. Two-dimensional approaches are applied through equivalent-single-layer (ESL) laminate theories [16], [17], with the appropriate shear correction factors [18]. ESL theories consider the displacements as continuous functions of the thickness coordinate, which cannot be satisfied at the CLT-concrete interface since a completely rigid connection is typically not achieved. Therefore, as shown in [19], the partial shear connection must be taken into account.

It was recently showed that Full-Layerwise Plate Theory of Reddy (FLWT) [16] can provide the accurate results for CLT panels in bending [15], [20], without compromising the accuracy of the 3D models. This theory incorporates the transverse normal stress σ_z and accounts for continuous transverse (interlaminar) stresses τ_{xz}, τ_{yz} and σ_z at layer interfaces within a CLT, without the use of shear correction factors.

The partial shear connection causes the interlayer slip at the CLT-concrete interface, which is usually accounted in plate kinematics by using Heaviside step function [19] or discontinuous interpolation functions. Therefore, the mentioned FLWT formulation is extended here to account for the interlayer slip. The slip moduli are incorporated by using the smeared approach, as distributed linear springs in three orthogonal directions at the interface. Based on the presented formulation, a family of layered quadrilateral isoparametric finite elements has been developed and implemented within the original object-oriented code FLWTFEM [21], [22] in MATLAB [23] and GiD [24] environments. The presented approach is validated against the available data in the literature, based on the zig-zag theory and results from the 3D models in Abaqus CAE [25].

Excellent agreement for static and dynamic simulations is obtained with computational cost savings. Finally, a parametric study on the influence of interlayer slip modulus on stress distribution in CCC is provided as a benchmark for future investigations.

2. LAYERWISE FORMULATION OF THE CCC KINEMATICS

In the paper, a CLT-concrete composite plate made of n_{CLT} orthotropic layers and a concrete topping is considered. The thicknesses of CLT and concrete are denoted as h_{CLT} and h_c, respectively (see

Figure 1), while the thickness of the k^{th} lamina is denoted as h_k ($k = 1, 2, \ldots, n$). The distributed loads q_t and q_b are associated to either top or the bottom surface of the composite plate.
The displacement field (u, v, w) of an arbitrary point (x,y,z) of the CLT-C composite is given as:

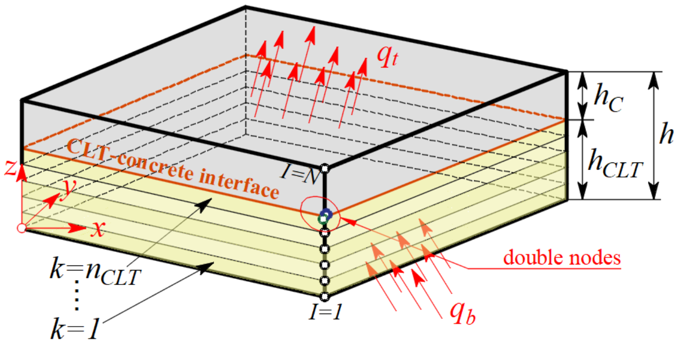

Figure 1. CLT-concrete composite plate with n_{CLT+1} material layers and $N=n_{CLT+3}$ interfaces (drawing by author).

$$u(x,y,z)=\sum_{I=1}^{N}U^I(x,y)\Phi^I(z),\quad v(x,y,z)=\sum_{I=1}^{N}V^I(x,y)\Phi^I(z),\quad w(x,y,z)=\sum_{I=1}^{N}W^I(x,y)\Phi^I(z) \quad (1)$$

where $U^I(x,y)$, $V^I(x,y)$ and $W^I(x,y)$ are the displacement components in the I^{th} interface (including the surfaces S_t and S_b) in three orthogonal directions, respectively, while N is the total number of numerical layers. $\Phi^I(z)$ are selected to be linear layerwise discontinuous functions of the z-coordinate [26], defined over the considered layer (above and below the interface I). This selection implicitly defines the interfaces (i.e. "numerical layers") in the planes between the material layers, including S_t and S_b. Note that in a CLT-concrete interface two mutually independent numerical layers are introduced, which enables including relative displacements between the CLT and concrete as the degrees of freedom. Piece-wise linear variation of all three displacement components through the plate thickness leads to the 3D stress description of all material layers, as given in [27].

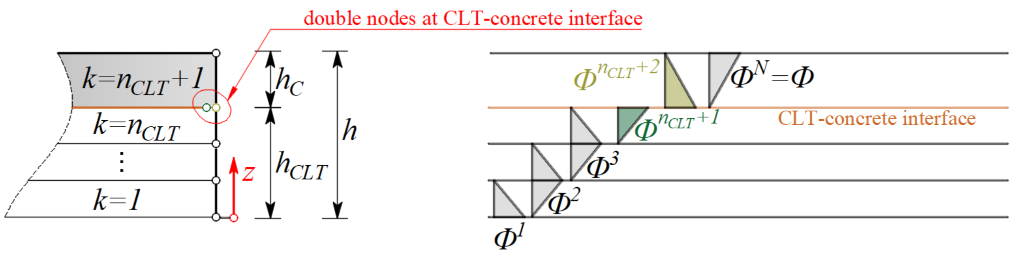

Figure 2. CLT-C composite with the interface at $z = h_{CLT}$ (left); linear layerwise functions $\Phi^I(z)$ with a discontinuity at CLT-concrete interface (right) (drawing by author).

Since only partial shear connection between CLT and concrete may be achieved, the interlayer slips Δu, Δv and Δw between the CLT and concrete arise [19]. They are introduced by means of different displacements in numerical layers located at the CLT-concrete interface (orange line in Figure 2a). By means of mathematical description, the inter-layer slip is enabled by using the discontinuous interpolation functions [26], as shown in Figure 2b.
The linear strain field is inherited from the displacement field (1) and the layerwise interpolation shown in Figure 2b. The explicit expressions of the strains (given in [16]) are extended by adding the adequate singularity terms related to the CLT-concrete interface (see [27] for details).
The stresses in the k^{th} interface may be computed from the well-known lamina 3D constitutive equations [15], [16], [27]. The interfacial stresses acting in the interface are proportional to the interlayer slip moduli K_i (note that for a very high selected value of K_z, Δw tends to zero which is a common value in CCC):

$$\tau_{xz}^{\text{int}}=K_x\Delta u(x,y,h_{CLT}),\quad \tau_{yz}^{\text{int}}=K_y\Delta v(x,y,h_{CLT}),\quad \sigma_z^{\text{int}}=K_z\Delta w(x,y,h_{CLT}) \quad (2)$$

Based on the above formulation, the family of 2D finite elements is derived by substituting an assumed interpolation of the displacement field (1) into the equations of motion of the FLWT. All displacement components are interpolated using the same degree of interpolation:

$$U^I(x,y)=\sum_{j=1}^{m}U_j^I\psi_j(x,y),\quad V^I(x,y)=\sum_{j=1}^{m}V_j^I\psi_j(x,y),\quad W^I(x,y)=\sum_{j=1}^{m}W_j^I\psi_j(x,y)\tag{3}$$

where m is the number of element nodes in the 2D element; U_j^I, V_j^I, W_j^I are the nodal values of displacements U^I, V^I and W^I, respectively, in the j^{th} node of the 2D element (representing the kinematics in the I^{th} interface), while $\psi_j(x,y)$ are the 2D Lagrange shape functions associated with the j^{th} element node.

In the element stiffness matrix, the additional terms K_x, K_y and K_z (corresponding to the interlayer slip moduli) are added in the rows and columns corresponding to the total of $6m$ nodal displacements in the CLT-concrete interface (the details may be found in [27]). The assumed piecewise linear interpolation of displacement field through the laminate thickness provides discontinuous stresses and strains across the interface between adjacent layers. Once the nodal displacements are obtained, the stresses at the top and bottom interface of every material layer (k) are computed from the constitutive relations (see [15]). The interlaminar stresses do not satisfy continuous distribution through the laminate thickness and they are further post-computed by assuming the quadratic distribution within each layer for every stress component. Note that the stress field acting in the CLT and concrete is enriched by adding the interface shear stresses, inherited from the displacement jumps Δu and Δv (Δw~0) and proportional to the slip moduli K_i [27].

3. BENDING ANALYSIS

An illustration example considers the rectangular CLT-concrete composite plate with dimensions $a \times b$ = 8×7 m [19], with two clamped edges, two free edges and a hinged point support at the corner (Figure 3, left). CLT is composed from seven layers, with a thickness of (2+4+2+4+2+4+2)=20cm, while a concrete topping thickness is 11cm. The CLT has the following material properties: E_L=12GPa, E_R=E_T=0.45GPa, G_{LR}=G_{LT}=0.70GPa, G_{RT}=0.06GPa and ν_{LR}=ν_{LT}=ν_{RT}=0.4, while the concrete properties are E_c=30GPa and ν_c=0.2. At the CLT-concrete interface, the interlayer slip moduli are K_x=10MPa and K_y=20MPa, which corresponds to a relative low level of the partial shear connection.

The plate is loaded with the distributed load at the top surface q_t = 10kN/m^2.

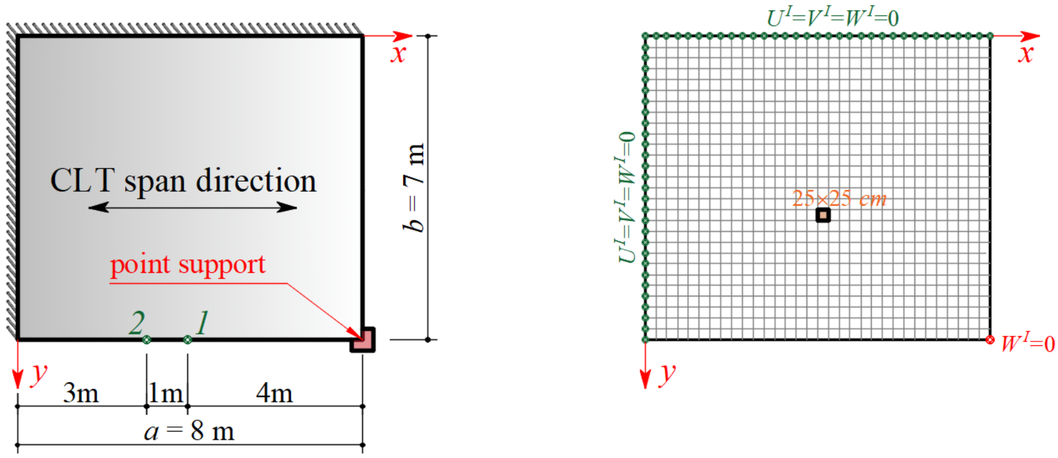

Figure 3. Layout (left) and finite element mesh (right) of the CLT-C composite (drawing by author).

The laminas are modelled as single numerical layers, while the concrete layer is modelled using two identical 5.5 cm thick layers. The discretization using 32×28 Q8R elements (8-node quadrilaterals with reduced integration) and boundary conditions are prescribed according to Figure 3, right.

The obtained results are compared against the data from [19], obtained using: (i) a continuum-based model in Abaqus using C3D20R elements and COH3D8 cohesive elements, and (ii) a higher-order zig-zag plate theory-based model, using Q8R finite elements with nine DOFs per node.

Figure 4 illustrates the distributions of the in-plane displacements u and v at point 1 ($4m$, $7m$) through the thickness of the considered CLT-concrete composite. The reference points 1 and 2 are selected along the free edge where the interlayer slips Δu and Δv reach their highest values. In addition, the locations are selected according to [19] in order to compare the results with the benchmark example.

The zig-zag shaped distribution of displacements, achieved by using FLWT, matches excellently with the reference data from the literature. The values of the inter-layer slips in both directions are captured accurately, proving that a proposed layerwise model is capable to accurately predict the kinematics of the CLT-concrete composite with partial shear connection.

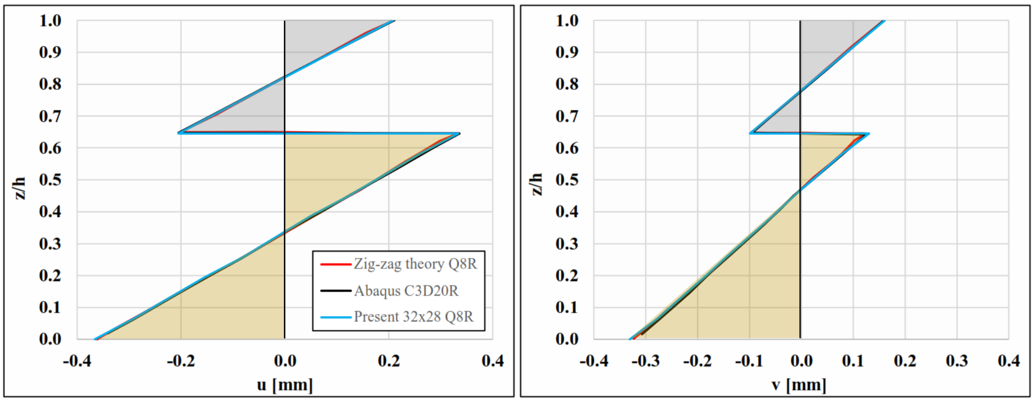

Figure 4. Distributions of the in-plane displacements u (left) and v (right) through the thickness of the CLT-concrete composite plate, in point 1 (4m, 7m), considering different models, for K_x = 10 MPa (drawing by author).

The strain field obtained by using FLWT is layerwise-linear, because of the layerwise linear expansion of displacements through the plate thickness. Normal strain ε_x in point 2 exhibits the laminate-specific zig-zag shape, with discontinuity at CLT-concrete interface. Excellent agreement is achieved when compared with the benchmark data (Figure 5, left). Jump in the normal strain ε_x is captured accurately, as well. Note that CLT and concrete act as almost mutually independent plates, which is visible from the *u*, *v* and ε_x distributions across CLT and concrete (Figures 4 and 5).
The proposed model accurately captures the layerwise-stepped distribution of transverse shear strain γ_{xz} (Figure 5, right), too. Transverse shear deformation is considerably higher in CLT when compared to concrete, due to the low shear moduli of timber when compared against the shear modulus of concrete G_c.

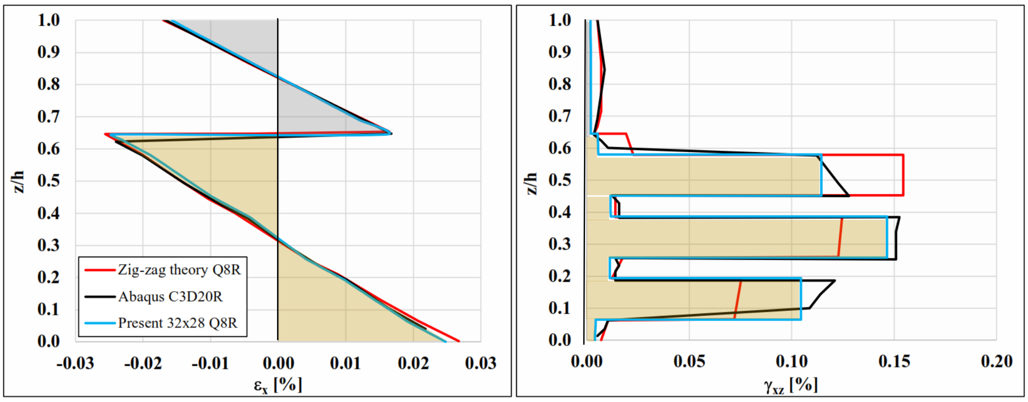

Figure 5. Distributions of the normal strain ε_x (left) and transverse shear strain γ_{xz} (right) in point 2 (3m, 7m) through the thickness of the CLT-concrete composite plate, considering different models, for K_x = 10 MPa (drawing by author).

4. FREE VIBRATON ANALYSIS

Free vibration study of the considered composite plate has been conducted next. For this purpose, only the self-weight of the structure has been considered as a mass source (ρ_{CLT} = 420 kg/m^3 and ρ_c = 2500 kg/m^3). The obtained results are again compared against the data [19].

Obtained natural frequencies with corresponding differences relative to the zig-zag theory [19] are given in Table 1. The results clearly show the high accuracy of the proposed model in the prediction of natural frequencies of CCC. The average relative difference when compared against the zig-zag theory [19] is -0.7%, which is almost negligible.

This completes the model validation by means of free vibration study, since excellent agreement is obtained when compared with the benchmark data. Therefore, the model accurately simulates the stiffness and mass distribution in CCC with interlayer slip.

Table 1. Natural frequencies of the CLT-concrete composite plate, considering different computational models and mesh densities, for K_x = 10 MPa

Mode	Zig-zag theory Q8R [19]	Abaqus C3D20R [19]	Present 32x28 Q8R
1	6.0 Hz	6.0 Hz	6.01 Hz
2	10.4 Hz	10.4 Hz	10.37 Hz
3	15.1 Hz	15.0 Hz	15.01 Hz
4	20.3 Hz	20.2 Hz	20.23 Hz
5	25.3 Hz	25.0 Hz	25.06 Hz
6	29.6 Hz	29.2 Hz	29.32 Hz
7	32.8 Hz	32.3 Hz	32.38 Hz
8	38.2 Hz	37.7 Hz	37.82 Hz
9	43.4 Hz	42.8 Hz	42.99 Hz
10	47.2 Hz	46.6 Hz	46.73 Hz

5. CONCLUSIONS

Starting from the full-layerwise-plate-theory-based FEM formulation of laminated composite plates with perfect bonding, the paper steps further to account for the possible interlayer slip at layer interfaces. This phenomenon is common in CLT-concrete and other plate-like composites with mechanical coupling devices.

The interface slip moduli are incorporated using the smeared approach, as distributed linear springs at the CLT-concrete interface. Interlayer slips are introduced by means of different displacements at the interface numerical layers. This is enabled by using the discontinuous interpolation functions of the thickness coordinate, previously developed for delamination studies. The strain field is enriched by adding the singularity terms related to the CLT-concrete interface. The stress field is enriched by adding the interface shear stress contributions inherited from the displacement jumps and proportional to the interlayer slip moduli.

Based on the presented formulation, Q8 layered quadrilateral isoparametric finite elements have been developed, which provide the complete stress/strain fields necessary for engineering failure analysis, delamination studies or stress-deformation state around point supports. The thickness coordinate is eliminated by the explicit integration of stress components; thus, a model formulation is reduced to the 2D (plate) model without compromising the accuracy and providing the computational cost savings when compared against the continuum-based (solid) models. Finally, the model allows the analysis of timber-concrete (TCC) or other plate-like layered composites with partial shear connection and arbitrary geometry.

From the conducted computational analysis, the following conclusions are derived:

- The zig-zag shaped distribution of displacement *u*, which is in accordance with the exact solution, is achieved using the proposed model. The values of the inter-layer slip are captured accurately in all directions, proving that a proposed model accurately predicts the kinematics of the CLT-concrete composite with partial shear connection.
- The model accurately predicts the layerwise-linear strain field. Normal strain ε_x exhibits the laminate-specific zig-zag shape, with discontinuity at CLT-concrete interface, while the

transverse shear strain γ_{xz} exhibits the jumps at layer interfaces. Excellent agreement is achieved when compared with the benchmark data.

- The model provided the high accuracy in the prediction of natural frequencies and mode shapes of CLT-concrete composite plate with various slip moduli, with the average relative difference less than 1%.

ACKNOWLEDGMENTS

The financial support of the Ministry of Science, Technological Development and Innovation of the Republic of Serbia, through the project 200092 is acknowledged. The author is grateful to Dr. Emilija Jočić for her contribution in development of the FLWTFEM software.

LITERATURE

[1] R. Brandner, G. Flatscher, A. Ringhofer, G. Schickhofer, and A. Thiel, "Cross laminated timber (CLT): overview and development," *Eur. J. Wood Wood Prod.*, vol. 74, pp. 331–351, 2016.

[2] G. Fink, J. Kohler, and R. Brandner, "Application of European design principles to cross laminated timber," *Eng. Struct.*, vol. 171, pp. 934–943, 2018.

[3] M. Shahnewaz, R. Jackson, and T. Tannert, "Reinforced cross-laminated timber-concrete composite floor systems," *Eng. Struct.*, vol. 291, Art. no. 116395, 2023.

[4] A. Dias, J. Skinner, K. Crews, and T. Tannert, "Timber-concrete-composites increasing the use of timber in construction," *Eur. J. Wood Wood Prod.*, vol. 74, no. 3, pp. 443–451, 2016.

[5] J. Kanócz and V. Bajzecerová, "Analysis of composite action of various mass timber structural panels with concrete layer," *Wood Res.*, vol. 63, pp. 1091–1100, 2018.

[6] M. Wang et al., "Experimental study on mechanical performance of shear connections in CLT-concrete composite floor," *Eng. Struct.*, vol. 269, Art. no. 114842, 2022.

[7] K. Q. Mai, A. Park, and K. Lee, "Experimental and numerical performance of shear connections in CLT–concrete composite floor," *Mater. Struct.*, vol. 51, pp. 1–13, 2018.

[8] J. Cao, H. Xiong, Z. Wang, and J. Chen, "Experimental investigation and numerical analysis for concrete-CLT connections," *Constr. Build. Mater.*, vol. 236, Art. no. 117533, 2020.

[9] J. Cao, H. Xiong, and J. Chen, "Mechanical characteristics and analytical model of CLT-concrete composite connections under monotonic loading," *Constr. Build. Mater.*, vol. 335, Art. no. 127472, 2022.

[10] G. Y. Jeong, V. S. Pham, and D. K. Tran, "Development of predicting equations for slip modulus and shear capacity of CLT–concrete composite with screw connections," *J. Build. Eng.*, vol. 71, Art. no. 106468, 2023.

[11] M. Milojević, V. Racic, and M. Nefovska-Danilović, "Uncertainty analysis of CLT floor vibrations due to inherent variability in structural properties," *J. Build. Eng.*, vol. 113, Art. no. 113725, 2025.

[12] V. Racic, "Emerging research on vibration serviceability assessment of pedestrian structures," *Build. Mater. Struct.*, vol. 66, no. 2, pp. 85–92, 2023.

[13] E. Ussher, K. Arjomandi, and I. Smith, "Status of vibration serviceability design methods for lightweight timber floors," *J. Build. Eng.*, vol. 50, Art. no. 104111, 2022.

[14] D. Casagrande, I. Giongo, F. Pederzolli, A. Franciosi, and M. Piazza, "Analytical, numerical and experimental assessment of vibration performance in timber floors," *Eng. Struct.*, vol. 168, pp. 748–758, 2018.

[15] M. Marjanović, N. Marković, E. Damnjanović, and R. Cvetković, "Three-dimensional stress analysis and design of cross-laminated timber panels using full-layerwise-theory-based finite element method," *Thin-Walled Struct.*, vol. 157, pp. 107–156, 2020.

[16] J. N. Reddy, Mechanics of Laminated Composite Plates and Shells: Theory and Analysis. Boca Raton, FL, USA: CRC Press, 2004.

[17] T. Furtmüller and C. Adam, "An accurate higher order plate theory for vibrations of cross-laminated timber panels," *Compos. Struct.*, vol. 239, Art. no. 112017, 2020.

[18] J. Whitney, "Shear correction factors for orthotropic laminates under static load," *J. Appl. Mech.*, vol. 40, no. 1, pp. 302–304, 1973.

[19] T. Furtmüller, "A finite element for static and dynamic analyses of concrete–cross-laminated timber composite plates," *Eng. Struct.*, vol. 328, Art. no. 119704, 2025.

[20] E. Jočić, M. Todorović, I. Glišović, and M. Marjanović, "An efficient computational model for progressive failure analysis of cross-laminated timber panels," *Arch. Appl. Mech.*, vol. 95, Art. no. 155, 2025.

[21] "FLWTFEM GitHub Repository," [Online]. Available: https://github.com/miregrf/FLWTFEM.

[22] M. Marjanovic, G. Meschke, and E. Damnjanovic, "Object-oriented framework for 3D bending and free vibration analysis of multilayer plates: Application to cross-laminated timber and soft-core sandwich panels," *Compos. Struct.*, vol. 255, pp. 112–159, 2021.

[23] MATLAB R2011b, The MathWorks, Inc., Natick, MA, USA, 2011.

[24] GiD Customization Manual, CIMNE – International Center for Numerical Methods in Engineering, Barcelona, Spain, 2016.

[25] ABAQUS User Manual 6.9, DS SIMULIA Corp., Providence, RI, USA, 2009.

[26] M. Rakocevic and L. Zugic, "A New Approach to the Embedding of Delamination in the Layerwise Theory of Laminated Composite Plates," *Symmetry*, vol. 14, Art. no. 1583, 2022.

[27] M. Marjanović, "Layerwise theory-based finite elements for static and dynamic analysis of CLT-concrete composites with partial shear connection," *Build. Mater. Struct.*, vol. 68, Art. no. 2500014M, 2025..